ACADEMIC PRESS

Available online at www.sciencedirect.com

SCIENCE DIRECT®

Journal of Sound and Vibration 267 (2003) 253–265

JOURNAL OF SOUND AND VIBRATION

www.elsevier.com/locate/jsvi

# Cyclic statistics in rolling bearing diagnosis

Li Li*, Liangsheng Qu

*Research Institute of Diagnostics and Cybernetics, Xian Jiaotong University, 710049 Xi'an, People's Republic of China*

Received 7 March 2002; accepted 8 October 2002

**Abstract**

Mechanical signals with amplitude modulated are characterized by periodic time-varying ensemble statistics and can be considered as cyclostationary. In this paper, the second order cyclic statistics, i.e. cyclic autocorrelation and cyclic spectrum, are introduced. A method of demodulation based on cyclic autocorrelation is derived from a signal model. The modulators and carrier are exhibited, respectively, in low- and high-frequency band of cyclic frequency domain. The three-dimensional spectral correlation figure, which represents cyclic frequency, frequency and spectral correlation strength simultaneously, is developed to express the demodulation results clearly. The method is tested by simulation signal and applied to diagnose rolling bearing faults. It obtained more information than other conventional methods, such as the frequency domain and the envelop detection. Furthermore, its effect is demonstrated by comparing with the wavelet envelope demodulation.


## 1. Introduction

The vibration signals of rotating machinery consist of random and periodic components. Their autocorrelation function exhibits time-varying, periodic and cyclostationary character. The periodic statistics contain the information of mechanical faults and often appear periodic correlated random impulses or modulation. Such a property can be found in the signals of faulty rolling bearings as well as faulty gears. As we know, the amplitude-modulated mechanical signals are difficult to be demodulated according to the ordinary theory based on the stationary assumption, especially when the modulators are weak and are buried in noise, so the stationary assumption has impeded the development of diagnosis technology.

*Corresponding author.
*E-mail address:* li7466@263.net (L. Li).

0022-460X/03/$ - see front matter 
doi:10.1016/S0022-460X(02)01412-8

Lately, the concept of cyclostationary statistics, or periodic time-varying ensemble statistics, is interested in machinery diagnosis. Cyclic statistics have been used as a tool for exploiting cyclostationarity in diagnostics practice. For example, the application of the degree of cyclostationarity to identify machine condition [1], the cyclic frequency found by spectral correlation graph to diagnose the machine fault [2]. However, these methods cannot be extended to solve general diagnostic problems, such as demodulation. The results are also too abstract to use in practice from the engineering point of view.

This paper discusses the formulas and tests based on the cyclic statistics. First, the second order cyclic statistics, or the cyclic autocorrelation and cyclic spectrum, are introduced. Then a mechanical signal model is developed to derive the signal demodulation formulas based on the cyclic autocorrelation. The signal demodulation technology can be applied to separate out the modulators effectively, especially for the weak modulators that cannot be detected by other conventional technologies, such as frequency domain and envelope detection. In order to exhibit the results clearly, a three-dimensional spectral correlation figure is developed, which located the modulators and carrier in low- and high-frequency band of cyclic domain, respectively. In applications, a simulated signal with amplitude modulated is used to verify the method. Then the mechanical signals of faulty rolling bearings (race spalling and rolling elements flaking) are diagnosed. In comparison with the wavelet envelop, the technology is proved to be more suitable to diagnose mechanical faults and can obtain more information.

## 2. Cyclic statistics and demodulation theory

In this section we present the theory of second order cyclic statistics and deduce demodulation formulas based on a signal model of amplitude modulated.

### 2.1. Cyclic autocorrelation

A zero-mean random process $x(t)$ generally possesses a time-varying autocorrelation

$$r_x(t,\tau) = E\{(x(t)x\,(t-\tau)\} \tag{1}$$

where $E\{\cdot\}$ is the mathematic expectation operator, $\tau$ is the time lag. If the autocorrelation is periodic with a period $t_0$, the resamples from $x(t)$ at, $\ldots, t-nt_0, \ldots, t-2t_0, t-t_0, t, t+t_0, t+2t_0, \ldots, t+nt_0, \ldots$, are satisfied ergodic condition and can be estimated with time average

$$r_x(t,\tau) = \lim_{N\to\infty} \frac{1}{2N+1} \sum_{n=-N}^{N} x(t+nt_0)x\,(t+nt_0-\tau). \tag{2}$$

Since $r_x(t,\tau)$ is periodic, it admits a Fourier series representation,

$$r_x(t,\tau) = \sum_{m=-\infty}^{\infty} r_x^{\alpha}(\tau)\mathrm{e}^{\mathrm{j}(2\pi/t_0)mt} = \sum_{m=-\infty}^{\infty} r_x^{\alpha}(\tau)\mathrm{e}^{\mathrm{j}2\pi\alpha t}, \tag{3}$$

where $\alpha = m/t_0$ and $m$ is an integer. $r_x(t,\tau)$ includes harmonics of the fundamental period $t_0$. Its Fourier coefficients $r_x^\alpha(\tau)$ can be given by

$$r_x^\alpha(\tau) = \frac{1}{t_0}\int_{-t_0/2}^{+t_0/2} r_x(t,\tau)\mathrm{e}^{-\mathrm{j}2\pi\alpha t}\,\mathrm{d}t. \tag{4}$$

When there exist more than one period $t_0$ in $r_x(t,\tau)$, formula (4) should be modified as

$$r_x^\alpha(\tau) = \lim_{t_n\to\infty}\frac{1}{t_n}\int_{-t_n/2}^{+t_n/2} r_x(t,\tau)\mathrm{e}^{-\mathrm{j}2\pi\alpha t}\,\mathrm{d}t = \left\langle r_x(t,\tau)\mathrm{e}^{-\mathrm{j}2\pi\alpha t}\right\rangle_t. \tag{5}$$

The function $r_x^\alpha(\tau)$, which represents the strength at frequency $\alpha$ in $r_x(t,\tau)$, is referred to as the cyclic autocorrelation. Clearly, it is not always reduced to zero for all non-zero $\alpha$ if $x(t)$ is cyclostationary. The set $\{\alpha : r_x^\alpha(\tau)\neq 0\}$ is referred to as the set of cyclic frequency. The non-zero cyclic frequencies characterize the cyclostationarity of signal.

The discrete form of the cyclic autocorrelation can be derived from (5)

$$r_x^\alpha(kT_s) = \left\langle r_x(nT_s, kT_s)\mathrm{e}^{-\mathrm{j}2\pi\alpha nT_s}\right\rangle_{nT_s}. \tag{6}$$

### 2.2. Cyclic spectrum

The cyclic spectrum can be obtained by means of Fourier transforming the cyclic autocorrelation

$$S_x^\alpha(f) = \int_{-\infty}^{\infty} r_x^\alpha(\tau)\mathrm{e}^{-\mathrm{j}2\pi f\tau}\,\mathrm{d}\tau. \tag{7}$$

Similarly, the discrete form $S_x^\alpha(kf_s)$ corresponds to $r_x^\alpha(kT_s)$. The cyclic spectrum, which is composed of spectral correlation functions, can detect the cyclic frequencies in signal [3]. A cyclic frequency has a large spectral correlation value. We will exhibit the results of the cyclic spectrum by means of the spectral correlation (SC) figure later, i.e., the three-dimensional figure of cyclic frequency–frequency–spectral correlation magnitude (SCM).

### 2.3. Demodulation theory

The demodulation theory is based on a most general mechanical signal model with amplitude modulated. It separates out the modulators in cyclic domain.

The signal model is

$$x(t) = \left(b + \sum_{i=1}^{N}\cos 2\pi f_{ci}t\right)\cos 2\pi f_0 t, \tag{8}$$

where $i = 1, 2, \ldots, N$ is the number of modulators, $f_{ci}$ and $f_0$ denote the modulator and the carrier, respectively, $f_0 > (5 \sim 10)\max(f_{ci})$, $b$ is a constant. The cyclic spectrum (single side) is as follows, its derivation in detail can be found in Appendix A.

$$S_x^{\alpha}(f) = \begin{cases} \dfrac{2b^2+b}{4}\delta(f+f_0) + \dfrac{b+1}{8}\sum_{i=1}^{N}\{\delta[f+(f_0+f_{ci})] + \delta[f+(f_0-f_{ci})]\} & \alpha = 0, \\ \dfrac{b^2}{4}\delta(f+f_0) & \alpha = 2f_0, \\ \dfrac{1}{16}\sum_{k=1}^{N}\delta[f+(f_0 \pm f_{ck})], & \alpha = 2f_0 \pm (f_{ci}+f_{ck}), \\ \dfrac{1}{16}\sum_{k=1}^{N}\delta[f+(f_0 \mp f_{ck})], & \alpha = 2f_0 \pm (f_{ci}-f_{ck}), \\ \dfrac{b}{8}\{\sum_{k=1}^{N}\delta[f+(f_0 \pm f_{ck})] + \delta(f+f_0)\}, & \alpha = 2f_0 \pm f_{ci}, \\ \dfrac{1}{16}\sum_{k=1}^{N}\delta[f+(f_0-f_{ck})], & \alpha = f_{ci}+f_{ck}, \\ \dfrac{1}{16}\sum_{k=1}^{N}\delta[f+(f_0+f_{ck})], & \alpha = |f_{ci}-f_{ck}|, \\ \dfrac{b}{8}\{\sum_{k=1}^{N}\delta[f+2(f_0-f_{ck})] + \delta(f+f_0)\}, & \alpha = f_{ci}, \\ 0 & \text{others.} \end{cases} \tag{9}$$

Here we only select positive value of $\alpha$ for mechanical engineering applications. Since $S_x^{\alpha}(f) \neq 0$ or $r_x^{\alpha}(\tau) \neq 0$ at the set of cyclic frequency $A = \{0,\ f_{ci}, f_{ci} \pm f_{ck}, 2f_0,\quad 2f_0 \pm f_{ci},\ 2f_0 \pm (f_{ci} \pm f_{ck})\}$ $(i, k = 1, 2 \ldots, N,$ number of modulators), so the demodulation based on the cyclic autocorrelation can be summarized as following:

(1) Since $f_0 > (5 \sim 10)\max(f_{ci})$, the components of signal can be separated into two parts in cyclic domain: the low-frequency band $A_1 = \{f_{ci},\ f_{ci} \pm f_{ck}\}$ and the high-frequency band $A_2 = \{2f_0,\ 2f_0 \pm f_{ci},\ 2f_0 \pm (f_{ci} \pm f_{ck})\}$. When $i = 1$, there is one modulator, the two parts in cyclic domain become $A_1 = \{f_c, 2f_c\}$ and $A_2 = \{2f_0,\ 2f_0 \pm f_c,\ 2f_0 \pm 2f_c\}$. Their effects are shown in Section 3.1.
(2) The low-frequency band only contains the information of modulators while the high-frequency band contains information of both carriers and modulators. Combining the two parts makes the demodulation process more reliable.
(3) When $b = 0$ or approaches zero, the low-frequency band $A_1 = \{f_{ci} \pm f_{ck}\}$, i.e., there exist intersections between modulators, the demodulation will become much more complex. In this case, combining the high-frequency band will be more effective.

Thus, the key demodulation operation is to search a set of cyclic frequencies of the modulators and to exhibit them correctly. This process is to scan in cyclic domain with a suitable cyclic frequency interval and find modulators. Fig. 1 gives the implementation diagram.

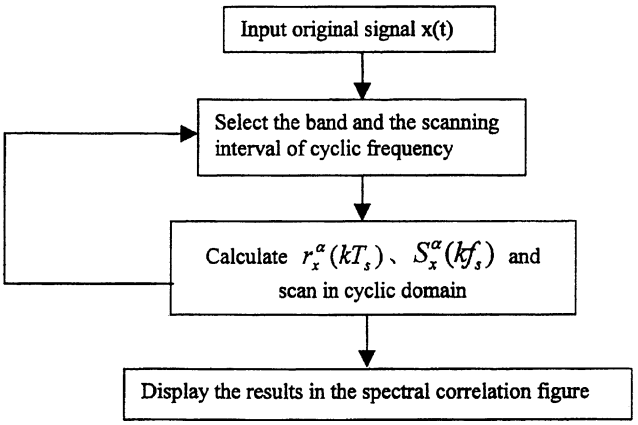


Fig. 1. The implementation diagram.

## 3. Applications

### 3.1. Simulation signal

The simulation signal we take is

$$x(t) = [1 + \cos(2\pi f_c t)]\cos(2\pi f_0 t),$$

where the modulator $f_c = 7$ Hz, the carrier $f_0 = 80$ Hz, the sample frequency is 1000 Hz and the number is 8192. The scanning interval in Fig. 2 is 1 Hz. Let $n$ and $k$ in Eq. (6) take 4096 and 1024, for each cyclic frequency (scanning interval) a set of cyclic autocorrelation data are obtained. Then applied discrete Fourier transformation (DFT) to the data, we can get its cyclic spectrum that is expressed by a continuous curve in the spectral correlation figure. The local maximum values in the figure may be corresponding to cyclic frequencies.

The demodulation results of the simulation signal are shown in Fig. 2, Fig. 2a and b exhibit the information in low- and high-frequency band of the cyclic domain. In Fig. 2a there are two peaks at $\alpha = 7$ Hz ($f_c$) and 14 Hz ($2f_c$). In Fig. 2b the peaks occur at $\alpha = 160$ Hz ($2f_0$), 153 Hz ($2f_0 - f_c$) and 167 Hz ($2f_0 + f_c$), 146 Hz ($2f_0 - 2f_c$) and 174 Hz ($2f_0 + 2f_c$), i.e., the intersections points among the modulators and the carrier. The results accord with conclusion (1) drawn in Section 2.3 and indicate that the modulators could be detected by scanning in the low-frequency band of cyclic domain.

### 3.2. Mechanical fault signals

In vibration signals of complex mechanical components, such as rolling bearings, the fault information is often contained in the modulators. When the modulators are weak and are buried in noise or other higher energy disturbances, the present conventional methods, such as FFT and envelope spectrum, can fail to detect them. However, in this case the demodulation based on the cyclic autocorrelation shows its advantages.

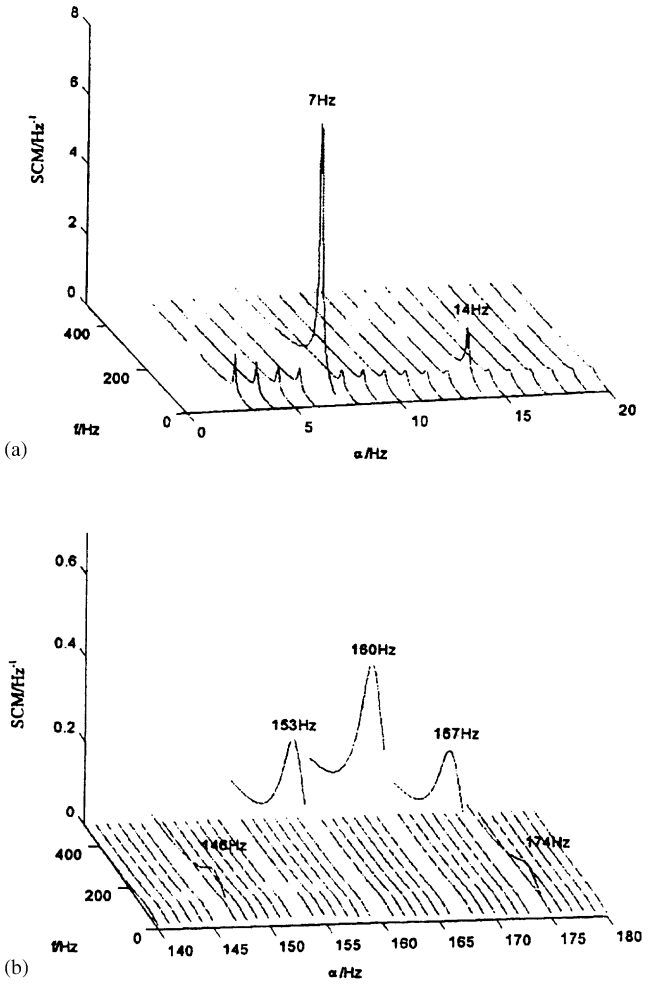


Fig. 2. The SC figure of the simulation signal: (a) scanning in low-frequency band and (b) scanning in high-frequency band.

The signals were sampled from the test rig, which consisted of a rotating shaft driven by an AC motor through a coupling and a gearbox. A rolling bearing of NSK308 held at the end of shaft. An accelerometer is attached to the bearing to pick up the signals. We can replace the bearing to test different kinds of faults. The related parameters are listed in Table 1.

The bearings faults create some sideband around the natural frequency of the bearing system. These faults characteristic frequencies are listed in Table 2 and their calculating formulas can be found in Appendix B. The demodulation based on the cyclic autocorrelation is applied to the four signals, which are normal, outer race fault, inner race fault and ball fault. The analysis frequency range is 3500–4500 Hz. In order to measure the characteristic frequencies of faulty bearings, different scanning intervals are selected and they are listed in Table 3. Two intervals in one figure can avoid unnecessary computation.

Table 1
The parameters of the test and the bearing itself

| The dimensions of the bearing | Natural frequency | Sampling frequency | Sampling number | Rotating frequency |
|---|---|---|---|---|
| Eight balls with 15 mm in diameter and 65 mm in the pitch diameter | 3827 Hz | 20 kHz | 8192 | 26.2 Hz |

Table 2
The diagnosable information using four methods

| Fault type | Characteristic frequency (Hz) | Time series method | Spectrum (Hz) | Wavelet envelope (Hz) | Cyclic statistics (Hz) |
|---|---|---|---|---|---|
| Normal bearing | No | No | No | No | No |
| Outer race spalling | 80.6 | 1 impulse | 80.5 | 80 | 80, 27 |
| Inner race spalling | 129.0 | 2–3 impulses | 26.7 | 129 | 27, 128 |
| Ball flaking | 53.7, 10 | No | No | No | 7, 107 |

Table 3
The scanning intervals in the SC figures

| | Fig. 4 | Fig. 5 | Fig. 6 | Fig. 7a | Fig. 7b |
|---|---|---|---|---|---|
| Origin: interval: end | 17:10:40<br>50:10:150 | 17:10:40<br>50:10:150 | 10:17:200 | 4:3:11<br>27:10:207 | 95:1:120 |

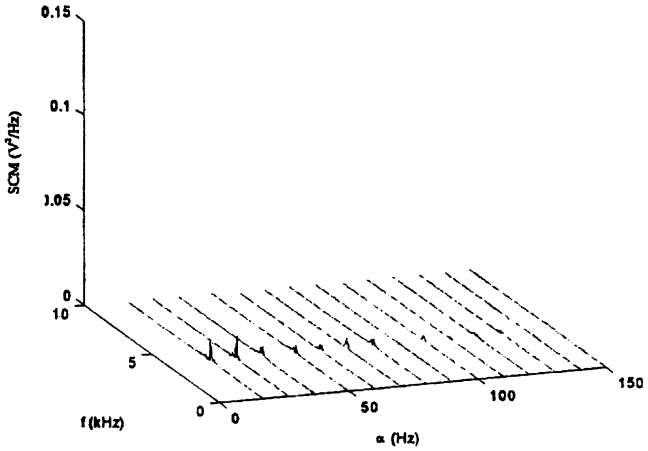


Fig. 3. SC figure of normal bearing.

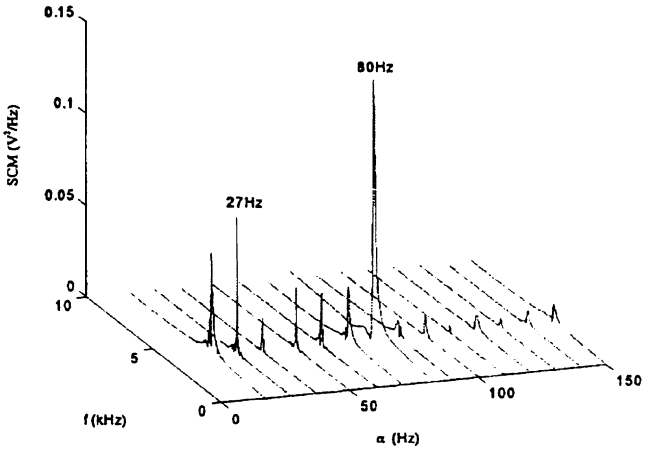


Fig. 4. SC figure of outer race spalling.

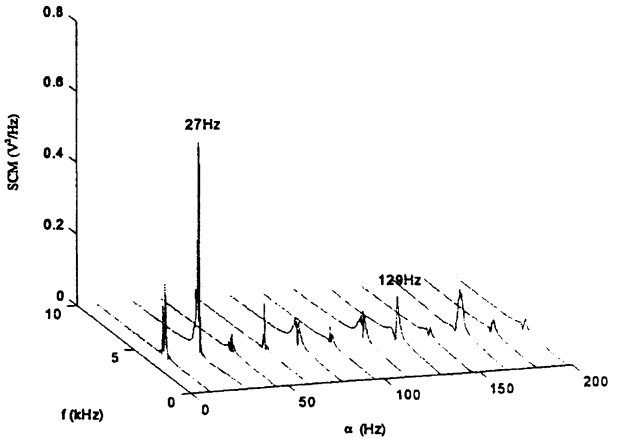


Fig. 5. SC figure of inner race spalling.

Fig. 3 is the spectral correlation (SC) figure of the normal bearing. There is no distinct peak, which means the signal is stationary. Figs. 4 and 5 show the spectral correlation figures of the bearing with outer race spalling and inner race spalling. Since the two kinds of faults create obvious impulses in the spectra, their fault features can be found easily with conventional methods; however, these methods cannot identify other weak modulators, such as 27 Hz in Fig. 4 and 129 Hz in Fig. 5.

Fig. 6a, the figure of the bearing with faulty rolling elements, exhibits two modulators 7 and 107 Hz, which are corresponding to the ball rotating frequency 10 Hz and impulse frequency 53.7 Hz. Since the frequencies are unstable due to the existed sliding effect inside the faulty bearing, they lead to irregular sideband around the natural frequency. So in this case the modulators are difficult to be detected using conventional methods. But the demodulation based on the cyclic autocorrelation can identify the weak modulators very efficiently. Because the

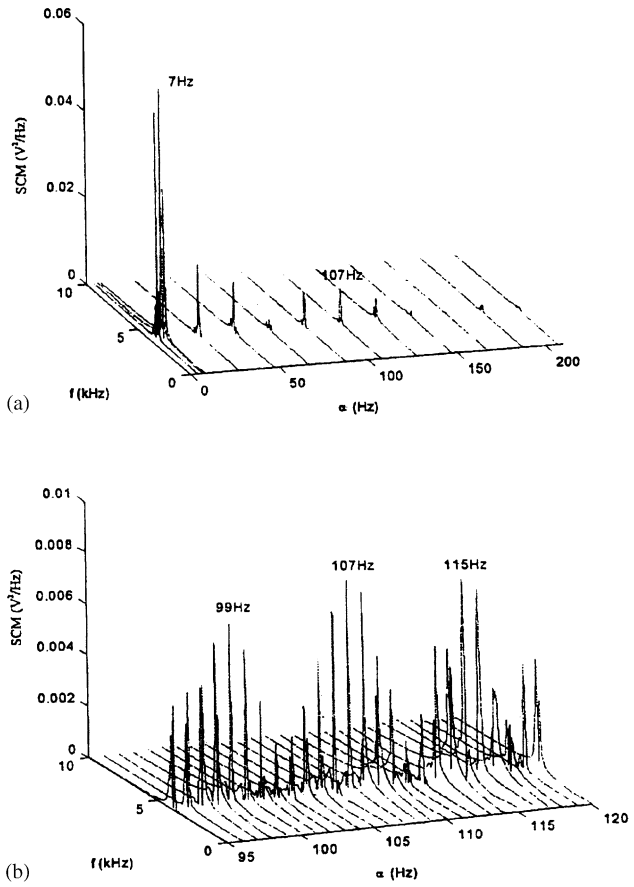


Fig. 6. The SC figure of ball flaking: (a) the figure of ball flaking and (b) the figure around 107 Hz.

bearing characteristic frequencies are based on the assumption of pure rolling motion, in reality, the sliding effect will cause the deviation of the calculated characteristic frequencies, especially for fault of rolling elements. This causes the deviation between the theoretical characteristic frequency 10 and 7 Hz. Fig. 6b is the figure scanning around 107 Hz. It exhibits the modulator of 8 Hz that verifies the existence of the sliding motion existing inside the bearing.

### 3.3. Comparison with wavelet envelope demodulation

We also give the results shown in Fig. 7 using the wavelet envelop [4] to analyze the above faulty signals. The wavelet envelope method utilizes the advantage of its band pass property and selects the optimal frequency band to detect the impulse of the signals. It separates out the modulators using the envelope demodulation. The method cannot detect the weak modulators due to the unclear impulse in time domain, such as the fault of rolling elements.

The analysis demonstrates that the demodulation method based on the cyclic autocorrelation can obtain more information and is more effective than other methods in bearing diagnosis. The

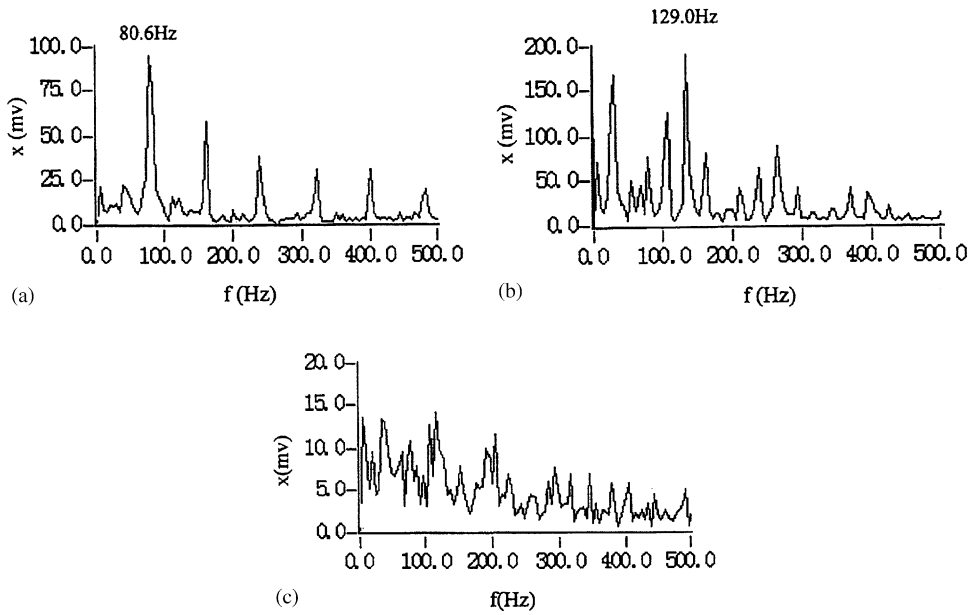


Fig. 7. Wavelet envelope spectra: (a) wavelet envelope spectrum of the outer race spalling, (b) wavelet envelope spectrum of the inner race spalling and (c) wavelet envelope spectrum of the ball flaking.

diagnotic information with time and frequency domain, wavelet envelope and cyclic statistics is listed in the Table 2.

## 4. Conclusions

The applications indicated that the second order cyclic statistics are suited to demodulate the mechanical signals and can extract the fault features effectively. The spectral correlation figure can exhibit the information clearly:

(1) The demodulation based on the cyclic autocorrelation can separate out the modulators and the carrier from the signals of amplitude modulated even for the weak modulators with the prerequisite of sufficient sample data. Because the noise is assumed a stationary random process, it will vanish after the operation of cyclic autocorrelation with large sample data. Ref. [5] indicates that the performance of suppressing noise by cyclic autocorrelation is directly proportional to $1/\sqrt{N}$, where $N$ is the sample number.

(2) The cyclic spectrum does not only contains the information in ordinary power spectrum ($\alpha = 0$) but also in cyclic statistics ($\alpha \neq 0$). The spectral correlation figure exhibits modulators in low-frequency band and both the carrier and modulators in high-frequency band of cyclic domain. Thus the modulators information is redundant and this makes the diagnosis more reliable.

(3) In comparison with the wavelet envelope for demodulated rolling bearing signal, the demodulation of the cyclic autocorrelation does not require to select the strict frequency band

and filter, thus its diagnostic function is stronger and more practical, especially the signal contains vague impulses (e.g., due to the fault on rolling elements). The cyclic statistics provide an effective tool to diagnose mechanical fault.

(4) Theoretically speaking, the peaks in the cyclic spectrum can only appear at the cyclic frequencies, but actually even $\alpha \neq 0$, there are lower peaks in certain range centering at $\alpha$, which does not affect the diagnosis result. Ref [6] discusses the problems deeply.

(5) It is important to select the scanning interval of cyclic frequency so that the cyclic characteristics can be detected. The minimum value of the interval should be larger than the frequency resolution [7]. When the characteristics are unknown in advance, the select and try process may be repeated several times.

## Appendix A

The derivation of the cyclic autocorrelation-based demodulation. The AM signal model is

$$x(t) = \left(b + \sum_{i=1}^{N} \cos 2\pi f_{ci} t\right) \cos 2\pi f_0 t.$$

For the sake of brevity, we reform the formulas as following:

$$x(t) = \frac{b}{2} e^{\pm j2\pi f_0 t} + \frac{1}{4} \sum_{i=1}^{N} (e^{\pm j2\pi f_{pi} t} + e^{\pm j2\pi f_{mi} t}),$$

$$e^{\pm j2\pi f t} = e^{+j2\pi f t} + e^{-j2\pi f t}, \quad f_{pi} = f_0 + f_{ci}, \quad f_{mi} = f_0 - f_{ci}.$$

Then the Fourier coefficients of $r_x(t,\tau)$ at cyclic frequency $\alpha$ are given by

$$\begin{aligned}
&\langle r_x(t,\tau) e^{-j2\pi\alpha t} \rangle_t \\
&= \left\langle \left[ \frac{b^2}{4} e^{\pm j2\pi f_0 \tau} + \frac{b^2}{4} e^{\pm j2\pi f_0 \tau} \times e^{\pm j4\pi f_0 \tau} + \frac{1}{16} \sum_{i=1}^{N} \sum_{k=1}^{N} e^{\pm j2\pi f_{pk} \tau} \left( e^{\pm j2\pi [2f_0 + (f_{ci} + f_{ck})]t} + e^{\pm j2\pi (f_{ci} + f_{ck})t} \right) \right. \\
&+ \frac{1}{16} \sum_{i=1}^{N} \sum_{k=1}^{N} e^{\pm j2\pi f_{mk} \tau} \left( e^{\pm j2\pi [2f_0 - (f_{ci} + f_{ck})]t} + e^{\pm j2\pi (f_{ci} - f_{ck})t} \right) \\
&+ \frac{1}{16} \sum_{i=1}^{N} \sum_{k=1}^{N} e^{\pm j2\pi f_{pk} \tau} \left( e^{\pm j2\pi [2f_0 - (f_{ci} - f_{ck})]t} + e^{\pm j2\pi (f_{ci} + f_{ck})t} \right) \\
&+ \frac{1}{16} \sum_{i=1}^{N} \sum_{k=1}^{N} e^{\pm j2\pi f_{mk} \tau} \left( e^{\pm j2\pi [2f_0 + (f_{ci} - f_{ck})]t} + e^{\pm j2\pi (f_{ci} + f_{ck})t} \right) + \frac{b}{8} \sum_{i=1}^{N} e^{\pm j2\pi f_{pi} \tau} \left( e^{\pm j2\pi (2f_0 + f_{ci})t} + e^{\pm j2\pi f_{ci} t} \right) \\
&\left. + \frac{b}{8} \sum_{i=1}^{N} e^{\pm j2\pi f_{mi} \tau} \left( e^{\pm j2\pi (2f_0 - f_{ci})t} + e^{\pm j2\pi f_{ci} t} \right) + \frac{b}{8} \sum_{i=1}^{N} e^{\pm j2\pi f_0 \tau} \left( e^{\pm j2\pi (2f_0 \pm f_{ci})t} + e^{\pm j2\pi f_{ci} t} \right) \right] e^{-j2\pi\alpha t} \Bigg\rangle_t.
\end{aligned}$$

Using the limit result [8]

$$\lim_{T\to\infty}\frac{1}{T}\int_{-T/2}^{T/2} e^{j2\pi ft}\,dt = \lim_{T\to\infty}\frac{\sin(2\pi fT/2)}{2\pi fT/2} = 0 \quad (f\neq 0) \tag{10}$$

we deduced the cyclic autocorrelation (for positive $\alpha$ value):

$$r_x^{\alpha}(\tau) = \begin{cases} \left(\frac{b^2}{2}+\frac{b}{4}\right)e^{\pm j2\pi f_0\tau} + \left(\frac{b}{8}+\frac{1}{8}\right)\sum_{i=1}^{N}\left(e^{\pm j2\pi(f_0+f_{ci})\tau} + e^{\pm j2\pi(f_0-f_{ci})\tau}\right) & \alpha = 0,\\ \frac{b^2}{4}e^{\pm j2\pi f_0\tau}, & \alpha = 2f_0,\\ \frac{1}{16}\sum_{k=1}^{N} e^{\pm j2\pi(f_0\pm f_{ck})\tau}, & \alpha = 2f_0\pm(f_{ci}+f_{ck}),\\ \frac{1}{16}\sum_{k=1}^{N} e^{\pm j2\pi(f_0\mp f_{ck})\tau}, & \alpha = 2f_0\pm(f_{ci}-f_{ck}),\\ \frac{b}{8}\left(\sum_{k=1}^{N} e^{\pm j2\pi(f_0\pm f_{ck})\tau} + e^{\pm j2\pi f_0\tau}\right), & \alpha = 2f_0\pm f_{ci},\\ \frac{1}{16}\sum_{k=1}^{N} e^{\pm j2\pi(f_0-f_{ck})\tau}, & \alpha = f_{ci}+f_{ck},\\ \frac{1}{16}\sum_{k=1}^{N} e^{\pm j2\pi(f_0+f_{ck})\tau}, & \alpha = |f_{ci}-f_{ck}|,\\ \frac{b}{8}\left(\sum_{k=1}^{N} e^{\pm j4\pi(f_0-f_{ck})\tau} + e^{\pm j2\pi f_0\tau}\right), & \alpha = f_{ci},\\ 0 & \text{others.} \end{cases}$$

Thus the cyclic spectrum (single side) is

$$S_x^{\alpha}(f) = \begin{cases} \left(\frac{2b^2+b}{4}\right)\delta(f+f_0) + \frac{b+1}{8}\sum_{i=1}^{N}\{\delta[f+(f_0+f_{ci})] + \delta[f+(f_0-f_{ci})]\}, & \alpha = 0,\\ \frac{b^2}{4}\delta(f+f_0), & \alpha = 2f_0,\\ \frac{1}{16}\sum_{k=1}^{N}\delta[f+(f_0\pm f_{ck})], & \alpha = 2f_0\pm(f_{ci}+f_{ck}),\\ \frac{1}{16}\sum_{k=1}^{N}\delta[f+(f_0\mp f_{ck})], & \alpha = 2f_0\pm(f_{ci}-f_{ck}),\\ \frac{b}{8}\{\sum_{k=1}^{N}\delta[f+(f_0\pm f_{ck})] + \delta(f+f_0)\}, & \alpha = 2f_0\pm f_{ci},\\ \frac{1}{16}\sum_{k=1}^{N}\delta[f+(f_0-f_{ck})], & \alpha = f_{ci}+f_{ck},\\ \frac{1}{16}\sum_{k=1}^{N}\delta[f+(f_0+f_{ck})], & \alpha = |f_{ci}-f_{ck}|\\ \frac{b}{8}\{\sum_{k=1}^{N}\delta[f+2(f_0-f_{ck})] + \delta(f+f_0)\}, & \alpha = f_{ci},\\ 0 & \text{others.} \end{cases}$$

## Appendix B

Cyclic autocorrelation calculation of bearing characteristic frequencies [9] (assuming pure rolling) are based on the following data:

Rotating frequency of the shaft: $f_r = 26.2$ Hz;
Number of balls: $n = 8$;
Pitch diameter: $D_p = 65$ mm;
Ball diameter: $d = 15$ mm.

The frequency characteristics for each kind of bearing fault are:

Outer race fault:
$$f_0 = \frac{n}{2}\left(1 - \frac{d}{D_p}\right) f_r = 80.6 \text{ Hz},$$

Inner race fault:
$$f_i = \frac{n}{2}\left(1 + \frac{d}{D}\right) f_r = 129.0 \text{ Hz},$$

Rolling ball fault:
$$f_b = \frac{D_p}{2d}\left(1 - \left(\frac{d}{D_p}\right)^2\right) f_r = 53.7 \text{ Hz},$$

Rolling ball rotation:
$$f_c = \frac{1}{2}\left(1 - \frac{d}{D_p}\right) f_r = 10.0 \text{ Hz}.$$

## References

[1] A.C. McCormick, A.K. Nandi, Cyclostationary in Rotating Machine Vibrations, Internationsl Conference by CWVA, Canada Machinery Vibration Association, Canada, 2001.
[2] R.B. Randall, J. Antoni, Separation of gear and bearing fault signals in helicopter gearboxes, fourth International Conference on Acoustical and Vibratory Surveillance Methods and Diagnosis Techniques, France, 2001.
[3] W.A. Gardner, Measurement of spectral correlation, IEEE Transactions on Acoustics, Speech and Signal Processing 34 (5) (1986) 1111–1123.
[4] D. Shi, M. Bao, L. Qu, Application of wavelet envelope analysis to rolling bearing diagnosis, China Mechanical Engineering 11 (12) (2000) 1382–1385.
[5] Y. Wang, Research on performance of suppressing noise by cyclic autocorreclation function, Journal of Data Acquisition & Processing 14 (2) (1999) 149–152.
[6] A.V. Dandawaté, G.B. Giannakis, Statistical tests for presence of cyclostationary, IEEE Transactions on Signal Processing 42 (9) (1994) 2355–2368.
[7] G.K. Yeung, W.A. Gardner, Search-efficient methods of detection of cyclostationary signal, IEEE Transactions on Signal Processing 44 (5) (1996) 1214–1223.
[8] H. Wang, in: Non-stationary Random Signal Analysis and Process, National Defense Industry Publishing Company, Beijing, 1999, pp. 315–320.
[9] L. Qu, Z. He, in: Machinery Fault Diagnostics, Shanghai Science and Technology Publishing Company, Shanghai, 1986, pp. 81–90.